Silica-Type Mesostructures from Block Copolymer Phases: Formation Mechanism and Generalization to the Dense Nanoparticle Regime

Anurag Jain and Ulrich Wiesner*

Department of Materials Science & Engineering, Cornell University, Ithaca, New York 14853

Received December 22, 2003; Revised Manuscript Received May 18, 2004

ABSTRACT: The present study elucidates the local structure and formation mechanism of a hybrid system based on poly(isoprene-*block*-ethylene oxide) diblock copolymers (PI-*b*-PEO) as structure directing agents for organically modified ceramic (ormocer) precursors, (3-glycidyloxypropyl)trimethoxysilane (GLYMO), and aluminum *sec*-butoxide ($Al(O^sBu)_3$). Employing results of pH measurements, solid-state NMR, scanning force microscopy, and mechanical properties analysis, it is shown that silica nanoparticles are an intermediate in the condensation process and that the final composites show structural heterogeneities within the PEO/inorganic containing domains of the hybrids. On the basis of the experimental results, a two-step model for the polymer−inorganic hybrid formation is developed. After sol−gel nanoparticle formation and subsequent mixing with the block copolymer, further condensation provides a locally heterogeneous PEO/inorganic domain conceptually similar to what is observed in alcogels, but replacing the solvent by PEO. Finally, implications of working in the high nanoparticle density regime with block copolymers or other amphiphiles for the generation of novel nanostructured, functional polymer−inorganic hybrid materials are discussed.

Introduction

The field of nanostructured organic−inorganic hybrid materials is one of the most promising and rapidly emerging research areas in materials chemistry. The October 2001 special issue of *Chemistry of Materials* nicely showcased recent progress in this multifaceted field through a number of selected short review articles summarizing the current state-of-the-art as well as selected original contributions highlighting recent achievements and exciting new forays.[1] In the May 2001 issue of the *MRS Bulletin* entitled "Hybrid Organic−Inorganic Materials" these materials were highlighted from an applications perspective. Topics covered through this vast field include bio- and biomimetic materials, composites, inorganic/organic networks, porous and self-assembled materials, and thin films. The special organization of dissimilar and usually incompatible components in organic−inorganic hybrid materials produces a wealth of novel structural features, physical properties, and complex functions, which arise from the synergistic interaction of the individual constituents.

To the best of our knowledge, it was in the second half of the 1990s that block copolymers were used for the first time as structure directing agents for silica-type ceramic materials.[2−6] In our group, research focuses on a particular hybrid system employing poly(isoprene-*block*-ethylene oxide) diblock copolymers (PI-*b*-PEO) as structure directing agents for organically modified ceramic (ormocer) precursors, (3-glycidyloxypropyl)trimethoxysilane (GLYMO) and aluminum *sec*-butoxide ($Al(O^sBu)_3$).[4] After epoxy ring opening triggered through the necessary presence of aluminum (Lewis acid), the 3-glycidyloxypropyl ligand of the silane precursor makes the inorganic mixture compatible with the PEO block of the block copolymer at any mole fraction. This compatibility allows for the selective swelling of the PEO block when a mixture of prehydrolyzed GLYMO/$Al(O^sBu)_3$ is added to PI-*b*-PEO, effectively increasing the PEO volume fraction with respect to the PI block. This results in a rational design of hybrid morphology based on current understanding of the phase behavior of block copolymers and copolymer−homopolymer mixtures.[7−12] In the meantime this approach (a) has led to the discovery of a new bicontinuous cubic structure,[13] (b) enabled the preparation of model nanocomposites with fillers of different shape and dimensionality,[14] (c) resulted in first demonstrations of unique property profiles in lithium ion battery applications,[15] (d) has been extended to mixed oxides and thin films,[16,17] and (e) has been generalized to high-temperature polymer-derived ceramics (PDCs) and extended amphiphilic dendrimers as structure directing agents.[18,19]

Here we take a closer look at the local structures and heterogeneities in the hybrids based on PI-*b*-PEO and GLYMO/$Al(O^sBu)_3$. In an earlier comprehensive solid-state NMR investigation of their local structure and dynamics, we showed that the hydrolyzed GLYMO/aluminum *sec*-butoxide mixture is intrinsically compatible with PEO, leading to a "two-phase" scenario.[20] No evidence for a PEO interphase between the inorganic hybrid and the organic PI phase (domains) was observed. This suggests that entropic effects drive the mixing of the aluminosilicate with the PEO. Despite the extent of this mixing, one-dimensional NMR spectra indicated that the local inorganic environments are not significantly perturbed by the incorporation of the aluminosilicate network into the PEO block of the copolymer. The presence of the block copolymer appears to have a negligible effect on the alkoxide condensation process. As an example, the relative populations of the different silicon T sites[21] in hybrids do not vary much as a function of inorganic content in the block copolymer nor do they differ significantly from those in the pure hydrolyzed GLYMO/aluminum *sec*-butoxide mixture (e.g., see Table 1 in ref 20). Intuitively, for a homogeneous mixing process one would rather expect that the incorporation of PEO chains into the inorganic network would lead to a significant suppression of the most highly condensed T^3 groups and populate the less condensed T^1 and T^2 groups. This effect should be strongest for small amounts of inorganic (e.g., micelles

10.1021/ma0359786 CCC: $27.50
Published on Web 07/02/2004

of inorganic/PEO in PI matrix morphology) and systematically weaken as the inorganic loading is increased (e.g., wormlike PI micelles in inorganic/PEO matrix morphology).

To understand why none of this is observed, one has to take a closer look at what is known about the sol−gel process of silica precursors and then apply this knowledge to the current PI-*b*-PEO plus GLYMO/Al(O^{s}Bu)$_3$ system. Two-step acid-catalyzed sol−gel polymerization of traditional silica sources has been shown to result in nanoparticles, which are mass fractals with a fractal dimension D_f around 2.0.[22] In the present paper, employing a combination of pH measurements and scanning force microscopy (SFM), we show that indeed silica nanoparticles are an intermediate in the condensation process. On the basis of these experimental results, revisiting the earlier NMR data and considering results of a nanoindentation study, a two-step model for the hybrid formation is developed. In the first step, very small silica-type nanoparticles are generated and mix with the PEO domains of the block copolymer. In the second step, these nanoparticles are cross-linked to form a dense network, which stays compatible with the PEO chains. Finally, implications of these findings for the generation of polymer−inorganic hybrid materials are discussed.

Experimental Section

Sol−Gel Process and Hybrid Synthesis. The poly(isoprene-*b*-ethylene oxide) diblock copolymer (PI-*b*-PEO) used for the block copolymer directed hybrid synthesis was synthesized using anionic polymerization techniques.[23] Gel permeation chromatography (GPC) was used to determine the molecular weight of the first block (polyisoprene, PI) and the dispersity of the block copolymer (see below). ^{1}H NMR was used to determine the chemical composition of the block copolymer and the microstructure of the PI block. The results were used to determine the overall molecular weight of the block copolymer. The molecular parameters were determined to be M_n = 21 900 g/mol, PDI = 1.04, and w_{PEO} = 0.15. The synthesis of the mesostructured hybrids was performed by a PI-*b*-PEO directed sol−gel synthesis described in ref 4. In this process the PEO block is swollen by prehydrolyzed ceramic precursors and acts as nanoreactors for their sol−gel synthesis. In a typical preparation, in a 20 mL vial, 0.5 g of PI-*b*-PEO was dissolved in a 1:1 weight ratio of chloroform and THF (10 g in total). The polymer solution was stirred rapidly for 1 h. Al(O^{s}Bu)$_3$ (1.4 g), GLYMO (5.3 g) (20:80 mol %), and an excess of KCl (40 mg) were heavily stirred for 1−2 min at 0 °C in a beaker before 0.27 g of 0.01 M HCl was added dropwise. After 15 min of stirring the sol at 0 °C followed by stirring for 15 min at RT, an additional 1.7 g of 0.01 M HCl was added dropwise and stirred for another 20 min. At every step of the prehydrolysis the pH of the solution was checked with pH paper. The clear sol was filtered through a 0.2 μm PTFE filter and added dropwise to the polymer solution. The organic−inorganic solution was stirred for 1 h before being transferred to a Petri dish and heated at 50 °C on a heating mantel for 1 h to evaporate off the solvents. The condensation products were removed from the film upon additional heating for 1 h at 130 °C in a vacuum oven, giving a film of 0.5−1 mm thickness. During the 1 h stirring step, samples were drawn from the mixture of block copolymer and prehydrolyzed sol−gel precursors at different times to examine the structure of the sol using SFM. After full condensation, the resulting nanostructured hybrids with PI as the majority phase were dispersed in an organic solvent to generate objects of different geometry.[24] Since PEO acts as an anchor block inside the ceramic phase, a thin layer of PI "hairs" covers the resulting nanoparticles. These "hairy" particles were then dispersed in toluene to make a 0.1 wt % solution. A Branson 250 sonifier (tip diameter $^7/_8$ in., 60% maximum output, 50% duty cycle) was used to assist complete particle separation.

Gel Permeation Chromatography. GPC measurements were performed in 98% THF and 2% *N*,*N*-dimethylacetamide[23] at room temperature using 5 μm Waters Styragel columns (10^3, 10^4, 10^5, 10^6 Å, 30 cm each; Waters Corp., Milford, MA) at a flow rate of 1.0 mL/min. A Waters 490 programmable multiwavelength UV diode array detector (operated at λ = 260 nm) and a Waters 410 RI detector operated at 25 °C were used. Raw data were processed using PSS-Win GPC V6.2 (Polymer Standards Service, Mainz, Germany) software.

Scanning Force Microscopy. For real-space imaging of the silica-type hybrids a Digital Instruments Nanoscope III multimode scanning probe microscope was utilized. The SFM was operated in tapping mode with TappingMode etched silicon probes (resonant frequency = 325 kHz, force constant = 37 N/m, tip radius of curvature = 10 nm; all values nominal) under ambient conditions. The SFM samples were prepared by dip-coating a freshly cleaved mica layer in the solution. Different protocols for selectively removing the organic components were used for ease of characterization. For imaging the structure of the precursors in solution before condensation the block copolymer was burnt away by heat treatment in a furnace at 400 °C. For imaging the nanoparticles, the polyisoprene hairs were etched away using UV-ozone treatment. The individual SFM images were corrected for nonlinearities in the scanner movement. A deconvolution of the tip shape from the images was not performed.

Small-Angle X-ray Scattering. Small-angle X-ray scattering (SAXS) experiments were performed on a Bruker-AXS NanoSTAR. The setup consisted of an X-ray source (Cu Kα, 1.54 Å) operated at 40 kV and 40 mA. Göebbel mirrors were used to focus the beam. A 2-D Hi-Star area detector at a sample-to-detector distance of 62.5 cm was used to record the scattering images. 2D images were integrated over the azimuthal angle (μ) to obtain one-dimensional intensity vs scattering plots.

Results and Discussion

To elucidate the local structure of hybrids based on PI-*b*-PEO and GLYMO/Al(O^{s}Bu)$_3$, the pH of the solution was checked at every step of the prehydrolysis. In all measurements, the pH stayed between 5.0 and 5.5. For such pH values and all other reaction conditions of our synthesis (see Experimental Section), it is expected that hydrolysis and condensation of the silica source proceed via the formation of nanoparticles (clusters) which are mass fractals; i.e., the larger they grow, the lower their density.[22,25,26] To examine the structure of constituents of the sol prior to transfer to a Petri dish where all volatile components are removed (see Experimental Section), scanning force microscopy (SFM) was employed. Indeed, nanoparticles were observed in samples that were made by dip coating a freshly cleaved mica layer at different times into a mixture containing block copolymer and prehydrolyzed sol. This is shown in Figure 1, where representative topographic images are displayed from samples obtained after stirring the mixed block copolymer and sol solution for $^1/_2$ h (a) and 1 h (b), respectively. Clearly in both cases nanoparticles are evidenced. Measuring height differences with the SFM between the particles and the substrate, the observed particles were found to be very small (<5 nm). This is consistent with the 2−4 nm clusters expected from a two-step acid-catalyzed sol−gel process.[27]

From these results it can be concluded that, at the stage in the synthesis procedure where solvents are evaporated off, the PI-*b*-PEO block copolymer is mixing with nanoscopic silica-type particles. Through solvent evaporation block copolymer mesophases are formed with morphologies that depend on the amount of sol added to the block copolymer, through mixing of the organically modified inorganic materials (referred to as the "inorganic") with the PEO block of the block

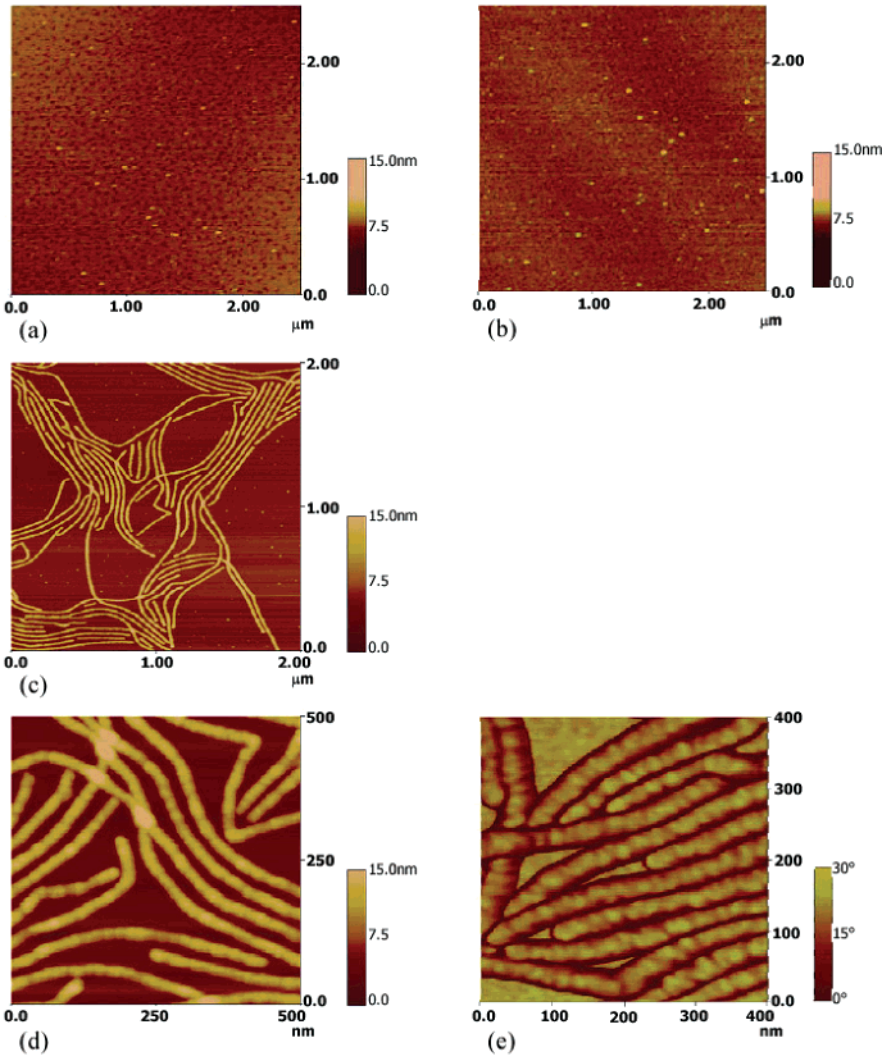

Figure 1. SFM images of the silica-type hybrid materials deposited on a mica surface. The samples were plasma-treated prior to imaging to remove the particle organic outer layer for easier imaging: (a) topographic image from a sample obtained after stirring the block copolymer and sol−gel precursor solution for $^1/_2$ h; (b) after stirring the same solution for 1 h; (c) topographic image of cylindrical hybrid nanoparticles obtained by redispersing the condensed bulk hybrids in toluene; (d) high-magnification topographic image of (c); (e) phase image of the cylindrical hybrid nanoparticles.

copolymer.[4,12] On the basis of the observation of nanoparticles as intermediates in the condensation process of the inorganic constituents, it is interesting to try to reveal the structure of the condensed gel that incorporates the PEO chains of the block copolymer. For the elucidation of structural aspects of the condensed gel, complementary to the information about the local structure as obtained by solid-state NMR experiments discussed in the Introduction, we performed high-magnification SFM imaging on isolated nanoobjects. They can be obtained through dissolution of the fully condensed bulk block copolymer−inorganic hybrid materials in toluene. Hybrid samples with a hexagonal morphology, i.e., with inorganic/PEO cylinders in a PI matrix, were chosen. The bulk morphology was confirmed using SAXS. As shown in Figure 2, the peak ratios of $\sqrt{1}$, $\sqrt{2}$, $\sqrt{3}$, and $\sqrt{7}$ for the pure block copolymer (lower trace) are indicative of a bcc morphology. When coassembled with inorganic components, peak ratios of $\sqrt{1}$, $\sqrt{3}$, and $\sqrt{7}$ were observed (upper trace) for the hybrid material consistent with a hexagonal morphology. Thus, a morphological transition from the pure polymer to the hybrid is induced as described earlier. When dissolved in toluene, these hybrids generate "hairy" nanoparticles that can be imaged by SFM

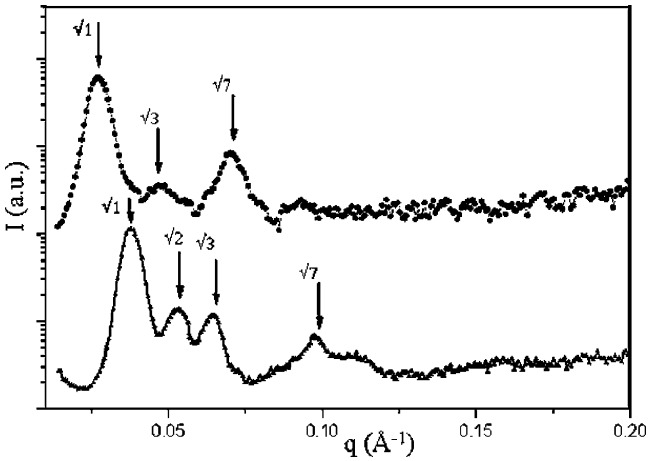

Figure 2. Small-angle X-ray scattering (SAXS) diffractograms of the pure PI-*b*-PEO block copolymer (▲) and the hybrid (●) derived from it by addition of sol−gel precursors. Data are shifted vertically for clarity. Peak positions with peak ratios consistent with a bcc (▲) and hexagonally packed cylinder structure (●) are indicated through ticks.

on mica.[24] A representative image is shown in Figure 1c. To enhance imaging capabilities, the polyisoprene

hairs associated with the nanoparticles were etched away using UV-ozone treatment. The core diameter of the rods calculated from SAXS data was found to be 17.6 nm, which matches closely to that observed in SFM images.[28] While individual rods of different lengths can easily be identified in Figure 1c, on this length scale morphological details of individual rods are difficult to see. We therefore performed scans at higher resolution. Representative results for high-resolution topographic and phase images are shown in parts d and e of Figure 1, respectively. While structural heterogeneities within the cylinders are already visible in the topographic image, they are much more pronounced in the phase image (Figure 1e). This figure reveals internal structure within the cylinders as evidenced by modulations in the elastic properties picked up by the SFM. Rather than a homogeneous polymer−inorganic network, the data suggest that the cylinder core consists of distinct regions with higher and lower network densities.

On the basis of these experimental results, a two-step model for the block copolymer−inorganic hybrid formation can now be developed. In the first step, nanoscopic (<5 nm) silica-type particles are formed through hydrolysis and condensation of the GLYMO and $Al(O^sBu)_3$ precursors. After mixing with the PI-*b*-PEO AB diblock copolymer solution, through evaporation of the volatile organic solvents they start to selectively swell the PEO block B. This scenario is depicted in Figure 3. Figure 3a schematically shows a particular block copolymer morphology with one block representing the minority PEO domain (white). When nanoparticles are mixed into the minority B domain, the resulting structural changes depend strongly on the particle size. As analyzed in detail, e.g., in recent work by Thompson and coworkers,[29] when the particles are small in comparison to the radius of gyration of the polymer chain, they can swell the polymer domain without significantly perturbing the polymer chain conformations. In this case the translational entropy of the particles dominates the behavior, leading to a uniform dispersion of the nanoparticles within the B (PEO) domain as depicted in Figure 3b. In contrast, when the particle size is of the order of the radius of gyration of the chains, incorporation into the B domain (PEO) significantly perturbs the chain conformations since B chains have to stretch to get around the spheres, resulting in a loss in chain conformational entropy. This is schematically depicted in Figure 3c. However, larger particles rather segregate into a particle-rich core which prevents the chain entropy penalty (at the expense of translational entropy of the particles), as shown in Figure 3d.

As discussed in the Introduction, from earlier NMR results we know that a segregation of a silica domain from a PEO domain does not occur in the PI-*b*-PEO/GLYMO/$Al(O^sBu)_3$ system at sufficiently high inorganic loading. From the present study it can be concluded that silica-type nanoparticles are formed as intermediates in the condensation process of the inorganic. This suggests that the scenario depicted in Figure 3b closely describes the hybrid formation process. The small nanoparticles only weakly perturb the PEO chain conformations, and their subsequent cross-linking through further condensation reactions leads to the final condensed state of the hybrid after additional thermal annealing for 1 h at 130 °C in a vacuum oven, leaving the PEO chains completely immersed in the organic/inorganic framework.

At this point it is interesting to revisit the solid-state ^{29}Si NMR results that indicated that the local inorganic environments are not significantly perturbed by the presence of the PEO chains. Irrespective of the PI-*b*-PEO/inorganic mixing ratio, ^{29}Si spectra showed about 30−35% T^3 groups, 49−54% T^2 groups, and 12−18% T^1 groups, with no obvious trends as a function of composition.[20] A condensation mechanism that is consistent with (i) these earlier NMR results, (ii) knowledge of the sol−gel process, and (iii) data presented in the present paper is the following: During prehydrolysis mass fractals in the form of silica-type nanoparticles are first formed. The two-step (hydrolysis and condensation) acid catalysis produces a distribution of T^1−T^3 species as expected for classic polycondensation of multifunctional monomers.[27] After mixing with the block copolymer solution as the solvents evaporate and hydrolysis and condensation proceed, the growing nanoparticles start to impinge each other. The open network structure generated in this way and filled with the PEO chains is likely to be qualitatively similar to what is typically observed during the formation of a conventional alcogel. After supercritical evaporation of the solvents the pore structure of the resulting aerogel has been nicely imaged in previous work by, e.g., Ruben et al.[30] Furthermore, at this point the number of additional bonds that need to be formed in order to generate a full three-dimensional network of nanoparticles is small compared to the number of bonds already present. This may explain why the relative populations of the different silicon T sites[21] in hybrids do not vary much as a function of inorganic content in the block copolymer and do not differ significantly from those in the pure hydrolyzed GLYMO/aluminum *sec*-butoxide mixture.

This suggested condensation mechanism is not only consistent with the small nanoparticles found in the SFM studies and the earlier NMR results but also with the heterogeneities as observed in the SFM phase image in Figure 1e. The sol−gel process is not expected to lead to a homogeneous distribution of nanoparticles but rather to an open network structure with free volume that can be occupied by the PEO chains. The nanoparticle-rich domains will be much harder than the PEO-rich domains. It can thus be assumed that it is these heterogeneities in the network density that are phase imaged by SFM (see Figure 1e). As a result of this discussion, the real situation of the nanoparticle/PEO coassembly is better represented by the schematic in Figure 3e than Figure 3b, which now shows the heterogeneities in the particle packing. It should be pointed out that in aerogels the pore sizes are in the range of 100 nm.[30] While the behavior of the present ormocer derived gels is qualitatively similar, the pore structure is expected to be significantly smaller, as indicated in Figure 3e. This is substantiated by recent solid-state NMR spin diffusion measurements on polymer electrolytes based on the same inorganic/PEO mixture but with the addition of a lithium salt.[15] These studies reveal heterogeneities with sizes of the mobile PEO domains down to a few nanometers at higher inorganic loadings.[31] More experimental work is needed, however, to elucidate this question in more detail in the present nanostructured block copolymer/inorganic hybrids in the future.

The suggested mechanism is also consistent with a recent study of the PEO/Glymo/$Al(O^sBu)_3$ hybrids conducted using nanoindentation.[32] As PEO content increased, the hardness and elastic modulus decreased nonlinearly, rapidly at first but with decreasing slope. This behavior is consistent with an interconnected silicate network, which becomes increasingly diluted as

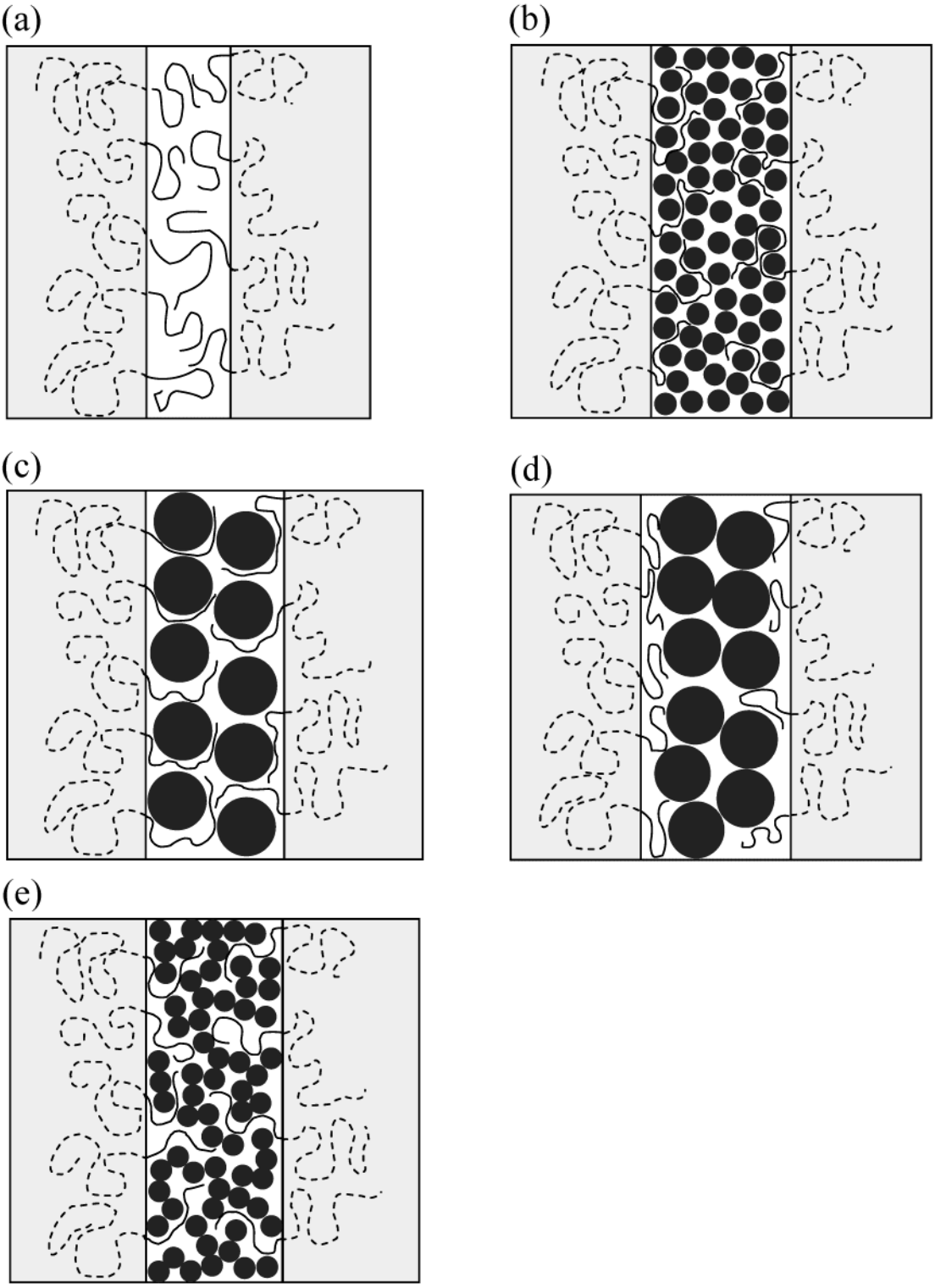

Figure 3. Schematics of local block copolymer structure without and with incorporation of nanoparticles at high density: (a) parent block copolymer, the solid chains forming the minority phase; (b) parent block copolymer selectively swollen with smaller nanoparticles at high density; the diameter of the particles is much smaller than the radius of gyration of the polymer leading to a homogeneous particle distribution with little effect on chain conformations; (c) parent block copolymer selectively swollen with larger nanoparticles; the diameter of the particles is of the order of the radius of gyration of the chains, thus leading to significant perturbations of the block chain conformations which are energetically unfavorable; (d) at high particle fractions in order to lower the chain conformational entropy the larger particles segregate into a central core; (e) same as (b) but with heterogeneous nanoparticle distribution as expected from the block copolymer directed sol−gel process of silica-type precursors.

PEO content increases (heterogeneous structure), as described by the present model.

Finally, the suggested mechanism and the resulting "open" structure is consistent with the observation of microporosity in the walls of mesoporous materials in the case where a PEO-containing block copolymer rather than, e.g., an ionic surfactant is used as the silica structure directing agent.[33] The microporosity in the wall is a direct result of the heterogeneity described above.

It is interesting to think about the broader implications of the suggested hybrid formation mechanism. Whereas most theoretical[29,34−39] and experimental[15,40−47] studies of block copolymers with nanoparticles up to the present date describe the low nanoparticle density regime, the present work strongly suggests that working in the high nanoparticle density regime might lead to some exciting new possibilities. As an example, it should be possible to generalize the hybrid formation mechanism beyond the present silica-based system. In principle, any inorganic material that (a) can be generated in small nanoparticle form, i.e., with particle dimensions significantly smaller than the radius of gyration of the polymer chains, and (b) can be made compatible (e.g., through the appropriate surface modifications) with one block of the block copolymer or any other amphiphile to provide nanostructurability through co-self-assembly should be applicable. If an appropriate surface chemistry allows further cross-linking of the inorganic, the nanostructure can additionally be fixed permanently. Thus, not only amorphous materials may be nanostructured through the help of block copolymers (as in the present example) but also crystalline inorganic materials. This may open an interesting playground for the design of novel nanostructured, functional hybrid materials.

Acknowledgment. Financial support of the National Science Foundation (DMR-0312913) and the Cornell Center for Materials Research (CCMR) (DMR-0079992) is gratefully acknowledged. We thank Prof. George W. Scherer (Princeton University) and Prof. Shefford P. Baker and Carlos B. W. Garcia (both Cornell University) for helpful discussions on the hybrid formation mechanism and Surbhi Mahajan (Cornell University) for help with the polymer synthesis. This work made use of the Cornell Center for Materials Research X-ray Diffraction Facility, supported through the National Science Foundation Materials Research Science and Engineering Centers Program (DMR-0079992).

References and Notes

(1) Special Issue: Organic−Inorganic Nanocomposite Materials; *Chem. Mater.* **2001**, *10*, 13.
(2) Bagshaw, S. A.; Prouzet, E.; Pinnavaia, T. J. *Science* **1995**, *269*, 1242.
(3) Göltner, C. G.; Antonietti, M. *Adv. Mater.* **1997**, *9*, 431.
(4) Templin, M.; Franck, A.; Du Chesne, A.; Leist, H.; Zhang, Y.; Ulrich, R.; Schädler, V.; Wiesner, U. *Science* **1997**, *278*, 1795.
(5) Zhao, D.; Feng, J.; Huo, Q.; Melosh, N.; Fredrickson, G. H.; Chmelka, B. F.; Stucky, G. D. *Science* **1998**, *279*, 548.
(6) Göltner, C. G.; Henke, S.; Weissenberger, M. C.; Antonietti, M. *Angew. Chem., Int. Ed.* **1998**, *37*, 613.
(7) Leibler, L. *Macromolecules* **1980**, *13*, 1602.
(8) Bates, F. S.; Fredrickson, G. H. *Annu. Rev. Phys. Chem.* **1990**, *41*, 525.
(9) Matsen, M. W.; Bates, F. S. *Macromolecules* **1996**, *29*, 1091.
(10) Hamley, I. W. *The Physics of Block Copolymers*; Oxford Science Pub.: London, 1998.
(11) Floudas, G.; Vazaiou, B.; Schipper, F.; Ulrich, R.; Wiesner, U.; Iatrou, H.; Hadjichristidis, N. *Macromolecules* **2001**, *34*, 2947.
(12) Simon, P. F. W.; Ulrich, R.; Spiess, H. W.; Wiesner, U. *Chem. Mater.* **2001**, *13*, 3464.
(13) (a) Finnefrock, A. C.; Ulrich, R.; Du Chesne, A.; Honeker, C. C.; Schumacher, K.; Unger, K. K.; Gruner, S. M.; Wiesner, U. *Angew. Chem., Int. Ed.* **2001**, *40*, 1208. (b) Finnefrock, A. C.; Ulrich, R.; Toombes, G. E. S.; Gruner, S. M.; Wiesner, U. *J. Am. Chem. Soc.* **2003**, *125*, 13084.
(14) Jain, A.; Gutmann, J. S.; Garcia, C. B. W.; Zhang, Y.; Tate, M.; Gruner, S. M.; Wiesner, U. *Macromolecules* **2002**, *35*, 4862.
(15) (a) Ulrich, R.; Zwanziger, J. W.; De Paul, S. M.; Reiche, A.; Leuninger, H.; Spiess, H. W.; Wiesner, U. *Adv. Mater.* **2002**, *14*, 1134. (b) Ulrich, R.; Zwanziger, J. W.; De Paul, S. M.; Richert, R.; Wiesner, U.; Spiess, H. W. *Polym. Mater. Sci. Eng.* **1999**, *80*, 610.
(16) (a) Garcia, C. B. W.; Zhang, Y.; DiSalvo, F.; Wiesner, U. *Angew. Chem., Int. Ed.* **2003**, *42*, 1526. (b) Garcia, C. B. W.; Zhang, Y.; Mahajan, S.; DiSalvo, F.; Wiesner, U. *J. Am. Chem. Soc.* **2003**, *125*, 13310.
(17) (a) Du, P.; Li, M.; Douki, K.; Li, X.; Garcia, C. B. W.; Jain, A.; Smilgies, D.-M.; Fetters, L. J.; Gruner, S. M.; Wiesner, U.; Ober, C. K. *Adv. Mater.* **2004**, in press. (b) Du, P.; Gutmann, J. S.; Simon, P. F. W.; Garcia, C. B. W.; Guarini, K.; Black, C. T.; Wiesner, U. *Polym. Prepr.* (*ACS, Div. Polym. Chem.*) **2002**, *43*, 438.
(18) Garcia, C. B. W.; Lovell, C.; Curry, C.; Faught, M.; Zhang, Y.; Wiesner, U. *J. Polym. Sci., Part B: Polym. Phys.* **2003**, *41*, 3346.
(19) Cho, B.-K.; Jain, A.; Mahajan, S.; Ow, H.; Gruner, S. M.; Wiesner, U. *J. Am. Chem. Soc.* **2004**, *126*, 4070.
(20) De Paul, S. M.; Zwanziger, J. W.; Ulrich, R.; Wiesner, U.; Spiess, H. W. *J. Am. Chem. Soc.* **1999**, *121*, 5727.
(21) For organosilicate species with a direct Si−C bond, the coordination of the silicon atom is described by the notation T^n ($n = 0$, 1, 2, or 3) where n is the number of bridging (Si−O−Si or Si−O−Al) oxygens. Different T^n species resonate at different ppm values in a ^{29}Si NMR spectrum.
(22) Meakin, P. *Annu. Rev. Phys. Chem.* **1988**, *39*, 237.
(23) Allgaier, J.; Poppe, A.; Willner, L.; Richter, D. *Macromolecules* **1997**, *30*, 1582.
(24) Ulrich, R.; Du Chesne, A.; Templin, M.; Wiesner, U. *Adv. Mater.* **1999**, *11*, 141.
(25) Iler, R. K. *The Chemistry of Silica*; John Wiley & Sons: New York, 1979.
(26) Bergna, H. E. *The Colloid Chemistry of Silica*, *Advances in Chemistry Series* 234; American Chemical Society: Washington, DC, 1994.
(27) Brinker, C. J.; Scherer, G. W. *Sol−Gel Science*; Academic Press: San Diego, 1990.
(28) Analyzing closely spaced cylinders in SFM images as in Figure 1c minimizes tip convolution effects.
(29) Thompson, R. B.; Ginzburg, V. V.; Matsen, M. W.; Balazs, A. C. *Science* **2001**, *292*, 2469.
(30) Ruben, G. C.; Hrubesh, L. W.; Tillotson, T. M. *J. Non-Cryst. Solids* **1995**, *186*, 209.
(31) Joo, C. G.; Bronstein, L. M.; Karlinsey, R. L.; Zwanziger, J. W. *Solid State NMR* **2002**, *22*, 235.
(32) Manuscript in preparation.
(33) Göltner, C. G. *Curr. Opin. Colloid Interface Sci.* **2002**, *7*, 173.
(34) Chervanyov, A. I.; Balazs, A. C. *J. Chem. Phys.* **2003**, *119*, 3529.
(35) Lee, J. Y.; Shou, Z.; Balazs, A. C. *Macromolecules* **2003**, *36*, 7730.
(36) Sevink, G. J. A.; Zvelindovsky, A. V.; Vlimmeren, B. A. C.; Maurits, N. M.; Fraaije, J. G. E. M. *J. Chem. Phys.* **1999**, *110*, 2250.
(37) Huh, J.; Ginzburg, V. V.; Balazs, A. C. *Macromolecules* **2000**, *33*, 8085.
(38) Lee, J. Y.; Baljon, A. R. C.; Sogah, D. Y.; Loring, R. F. *J. Chem. Phys.* **1987**, *112*, 9112.
(39) Groenewold, J.; Fredrickson, G. H. *Eur. Phys. J. E* **2001**, *5*, 171.
(40) Sankaran, V.; Cummins, C. C.; Schrock, R. R.; Cohen, R. E.; Silbey, R. J. *J. Am. Chem. Soc.* **1990**, *112*, 6858.
(41) Chan, Y. N. C.; Schrock, R. R.; Cohen, R. E. *Chem. Mater.* **1992**, *4*, 24.
(42) Moffitt, M.; McMahon, L.; Pessel, V.; Eisenberg, A. *Chem. Mater.* **1995**, *7*, 1185.
(43) Spatz, J. P.; Roescher, A.; Sheiko, S.; Krausch, G.; Möller, M. *Adv. Mater.* **1995**, *7*, 731.
(44) Antonietti, M.; Wenz, E.; Bronstein, L.; Seregina, M. *Adv. Mater.* **1995**, *7*, 1000.
(45) Clay, R. T.; Cohen, R. E. *Supramol. Sci.* **1995**, *2*, 183.
(46) Kane, R. S.; Cohen, R. E.; Silbey, R. *Chem. Mater.* **1996**, *8*, 1919.
(47) Bockstaller, M. R.; Lapetnikov, Y.; Margel, S.; Thomas, E. L. *J. Am. Chem. Soc.* **2003**, *125*, 5276.

MA0359786